

Molecular dynamics simulation of model room temperature ionic liquids with divalent anions

S G Raju & S Balasubramanian*

Chemistry and Physics of Materials Unit, Jawaharlal Nehru Centre for Advanced Scientific Research,
Jakkur, Bangalore 560 064, India

Email: bala@jncasr.ac.in (SB)/ raju@jncasr.ac.in (SGR)

Received 22 January 2010; revised and accepted 22 March 2010

Room temperature ionic liquids contain molecular ions which are, in general, monovalent. In the present work, the intermolecular structure, dynamics and intermediate range structure in a model ionic liquid, whose cation and anion are mono- and di-valent respectively, have been explored. Charge compensation is met by doubling the mole fraction of the cations in the sample. Through coarse grained molecular dynamics simulations, an enhancement of electrostatic interactions in the liquid which leads to greater ordering and sluggish dynamics, relative to traditional room temperature ionic liquids, has been observed. The nanoscale heterogeneity inherent to room temperature ionic liquids is also further increased in these divalent systems.

Keywords: Theoretical chemistry, Ionic liquids, Molecular dynamics, Simulation studies, Divalent ionic liquids

Room temperature ionic liquids (RTIL)¹⁻⁷ are a class of substances containing only ions and are liquid at or below 100 °C. These compounds are generally composed of an organic cation and an organic or inorganic anion. Due to the presence of a bulky and asymmetric cation, their crystalline forms have lower cohesive energies compared to purely inorganic salts such as NaCl, BaCl₂ etc. The liquid state is thus favored at ambient conditions on free energy terms. Since the constituents of ionic liquids interact via strong and long ranged Coulombic forces, they exert practically no vapor pressure. They can be used as solvents for a wide range of polar and non-polar solutes. A combination of different cations and anions in RTIL can, in principle, lead to a large number of compounds with varied physical and chemical properties. Many reactions have been shown to be influenced when an ionic liquid is used as a solvent⁸⁻¹⁰. Apart from neat ionic liquids, several studies have been conducted on aqueous solutions of ionic liquids¹¹⁻¹⁶ and of micellar ionic liquid solutions¹⁷⁻¹⁹.

Molecular dynamics simulations²⁰⁻²⁵, fluorescence spectroscopy^{26,27} and X-ray scattering experiments²⁸⁻²⁹ have shown that RTILs, especially the ones with imidazolium based cations, exhibit nanoscale phase separation. In these systems, the anion and imidazolium ring of the cation constitute the polar moieties while the alkyl chain on the cation is non-

polar. The non-polar entities aggregate and so do the polar ones. This leads to microphase segregation in the otherwise isotropic and homogeneous liquid. The spatial heterogeneity is understood to be due to the competition between short-range interactions between the tail groups and the long-range Coulomb interactions between the head groups (of cations) and the anions²³. As the length of the alkyl chain on the cation is increased, spatial heterogeneity increases due to enhancement in the van der Waals (vdW) interactions between the alkyl chains.

RTILs typically contain monovalent ions and the mole fraction of cations (or anions) is half; the effect of divalent anions such as sulfate (SO₄²⁻), thiosulfate (S₂O₃²⁻), sulfite (SO₃²⁻), chromate (CrO₄²⁻), dichromate (Cr₂O₇²⁻), carbonate (CO₃²⁻) and oxalate (C₂O₄²⁻) on the structural and dynamical properties of ionic liquids is, to our knowledge, unexplored. Doubling the charge on the anion needs to be necessarily compensated by doubling the mole fraction of the imidazolium cations in the ionic liquid, for reasons of charge neutrality. This would increase electrostatic interactions. The consequence of these changes on the properties of the ionic liquid is the object of the current study. We explore this problem using coarse grained molecular dynamics simulations, an apt tool to study the evolution of microheterogeneity in complex systems.

Simulation Studies

We have earlier developed a coarse grained model for 1-methyl-3-alkylimidazolium hexafluorophosphate $[C_n\text{mim}][PF_6]$. The model has been employed successfully to study the microheterogeneity in RTILs as a function of the alkyl group length²⁵, the effect of shear on the structure³⁰, and recently, to study the spontaneous formation of a lamellar phase in ionic liquids of the type, $[C_nC_n\text{im}][PF_6]$ ³¹. A schematic depicting the correspondence between the atomistic and coarse grain representations of the ions is shown in Fig. 1. The cation has six beads and the anion has one bead. The cation contains a positively charged "head" made of three atoms: I1, I2 and I3. This is equivalent to the imidazolium ring in the atomistic representation. CM and CT are the beads for the alkyl chain on the cation and PF is the bead representing the divalent anion. Information regarding the form of the interaction potential is explained in an earlier work²⁵. Intramolecular terms include harmonic bond stretches and angle bends. Coulombic and 9-6 Lennard-Jones interactions mediate non-bonded neighbours. Since we wanted to simulate a RTIL with divalent anion, we have doubled the charge on the anion and considered twice the number of cations (monovalent) as of anions. The charge on a monovalent anion in our model is set to $-0.8 e$ (ref. 25) and thus the divalent anion studied herein carries a charge of $-1.6 e$. The overall charge on the cation is $+0.8 e$. The 9-6 (softer when compared to Lennard-Jones) interactions were the same as that for the PF_6^- anion. The interaction model is not specific to any particular divalent anion; our aim in this work is to capture the generic features of intermolecular (and intermediate range) structure that is brought about by the introduction of divalent anions in RTILs.

Classical molecular dynamics (MD) simulations were performed using the LAMMPS code³². A time step of 4 fs was used to integrate the equations of motion. Non-bonded interactions were treated with a spherical cutoff of 1.5 nm, and the long range part of the electrostatic interactions was treated using the particle-particle particle mesh Ewald method. The system consists of a total of 2600 beads with 400 $[C_{10}\text{mim}]^+$ cations and 200 anions. A simulation box containing randomly arranged coordinates of these ions was taken as the initial configuration and the system was equilibrated under constant NPT conditions for 1.2 μs . Later, the system was simulated

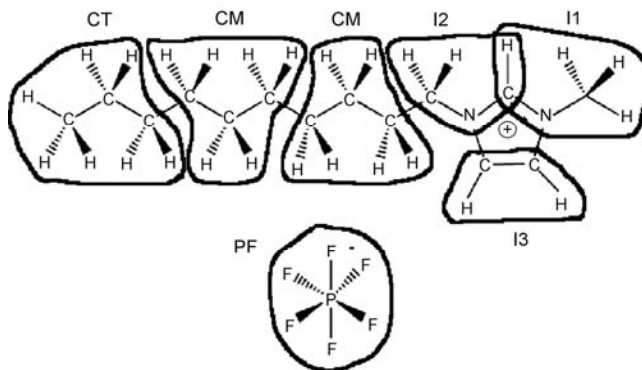


Fig. 1 — Schematic representation of $[C_{10}\text{mim}][PF_6]$ illustrating the mapping of atoms to coarse grain beads.

under constant NVT conditions for 320 ns. Coordinates stored every 200 ps were later used for analysis. The temperature of the system was maintained at 300 K using a Nose-Hoover thermostat. The final box length of the divalent system was 55.1 Å. Pair correlation functions between the beads of the ions have been calculated using bin width of 0.01 Å. The partial structure factors were calculated from these pair correlation functions using the following relationship (Eq. 1),

$$S_{\alpha\beta}(q) = \delta_{\alpha\beta} + 4\pi\sqrt{\rho_{\alpha}\rho_{\beta}} \int_0^{\infty} r^2 [g_{\alpha\beta}(r) - 1] \frac{\sin(qr)}{(qr)} dr \quad \dots(1)$$

where $\rho_{\alpha} = \frac{N_{\alpha}}{V}$, N_{α} is the number of beads of type α

and V is the volume of the system. The upper limit in the integral is replaced by half of the simulation box length. The total neutron scattering function is obtained from these partial functions using appropriate scattering lengths as given by Eq. (2),

$$S(q) = \sum_{\alpha} \sum_{\beta} c_{\alpha} c_{\beta} \frac{f_{\alpha}(q) f_{\beta}(q)}{\langle f(q) \rangle^2} S_{\alpha\beta}(q) \quad \dots(2)$$

where c_{α} is the concentration of bead type α in the system, f_{α} is the scattering length of bead α and $\langle f(q) \rangle = \sum_{\alpha} c_{\alpha} f_{\alpha}(q)$.

To understand the effect of increase in charge density on anion, we have also analyzed a system with the same cation but with a monovalent anion (PF_6^-). This system has equal number of cations and anions (3375 ions of each kind, same as reported in our earlier work²⁵). We compare the results of this system with the one containing the divalent anion. In

the rest of the article, we refer to the system containing monovalent anion as system A and the one containing divalent anions as system B.

Results and Discussion

Radial distribution function

The radial distribution functions (RDFs) between the polar sites of the ions is shown in Fig. 2. It

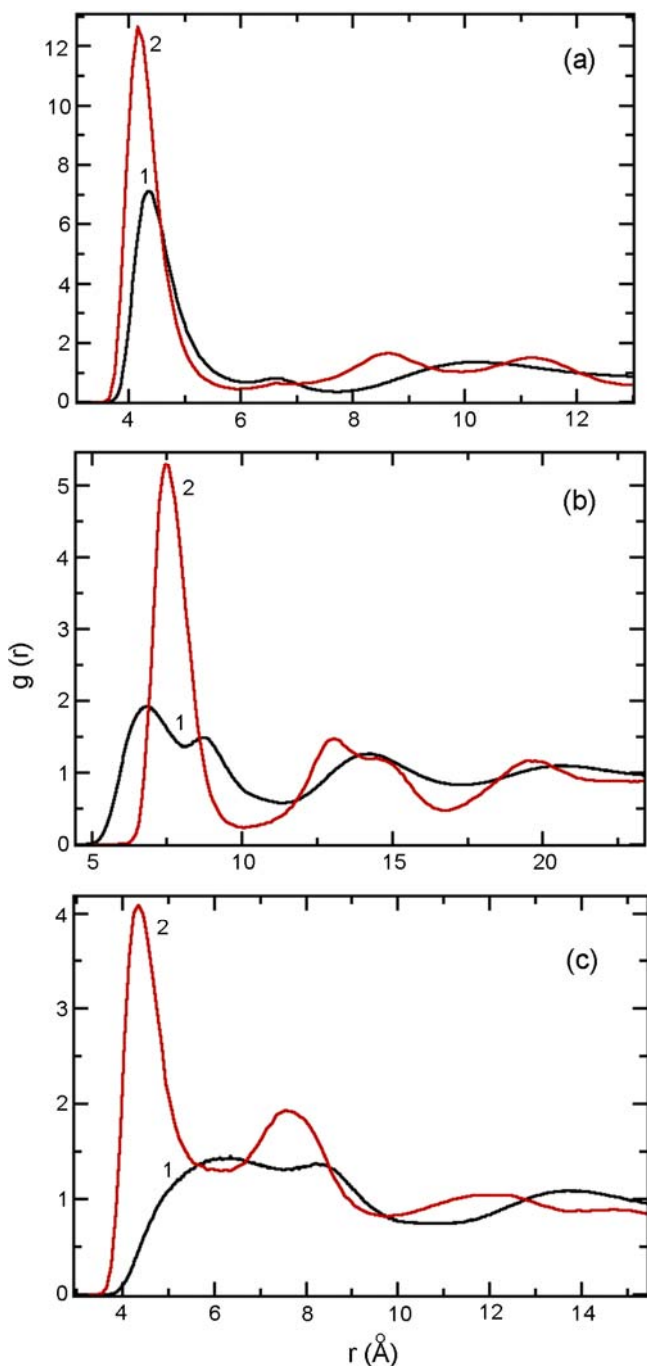


Fig. 2 — Comparison of RDF between systems A (monovalent anion) and B (divalent anion). [a, I1-PF; b, PF-PF; c, I1-I1 bead pairs. 1, system A; 2, system B].

compares the RDFs between system A and system B for (a) head-anion (I1-PF), (b) anion-anion (PF-PF) and (c) head-head (I1-I1). A large increase in the intensity of the first peak in all the RDFs is seen for system B. Also, its position shifts to lower distances in the case of head-anion and head-head correlation functions, while it shifts to the right for the anion-anion RDF. The latter is due to the increased value of charge on the anion. An important observation is the large increase in the peak height of head-head RDF and the closer approach of imidazolium rings of neighbouring cations in system B relative to that in system A. It implies ordering of the cations and possible stacking of the adjacent ring planes. The increase in the peak height of the head-anion RDF is due to the enhanced Coulombic interaction between these two groups in view of the anion in system B containing twice the charge as that in system A.

These three RDFs provide us valuable information about the local structure in the polar regions of the IL. They strongly indicate that the increase in charge density of the anion has led to an increase in the

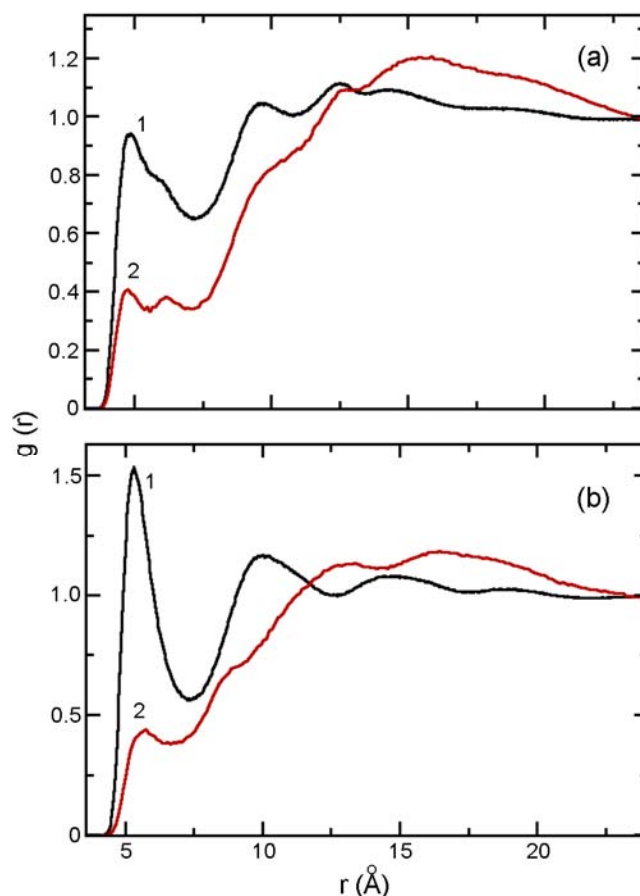


Fig. 3 — Comparison of RDFs between systems A and B. [a, I1-CT; b, PF-CT bead pairs. 1, system A; 2, system B].

strength between the sites constituting the polar regions. There is a similar increase in the intensity of the first two peaks in the RDF between the alkyl tails of the cation in system B as compared to that in system A (Fig. 3a). Thus, the non-polar region of the IL (constituted by the alkyl tails) is also more structured in system B than in system A. We now look at the RDFs between head-tail (II-CT) and anion-tail (PF-CT) in Fig. 3. There is a large decrease in intensity of the first two peaks for system B, indicating that the correlation between a polar and a non-polar site is drastically reduced in divalent anion based ionic liquid as compared to the monovalent one. In summary, the increase in the charge density of the anion leads to a more ordered local structure.

Structure factor

While structural order at near neighbour distances can be probed in real space readily using radial distribution functions, such ordering at the intermediate to long range distances is often easier to discern in reciprocal space. Calculation of the structure factor, $S(q)$, is thus crucial in order to study the microheterogeneity in any system, and in particular in ionic liquids. A study of the total structure factor (TSF) and the contributing partial structure factors (PSFs) will shed some light on the effect of increase in charge density of anion on the intermediate range spatial correlations. Figure 4 compares the TSF between systems A and B. System A exhibits peaks at 0.28 \AA^{-1} , 0.97 \AA^{-1} and 1.44 \AA^{-1} corresponding to real space correlation lengths of 22.4 \AA , 6.5 \AA and 4.4 \AA . System B shows a peak at 0.28 \AA^{-1} whose intensity is much larger than that in system A. The peak at 0.28 \AA^{-1} (correlation length of

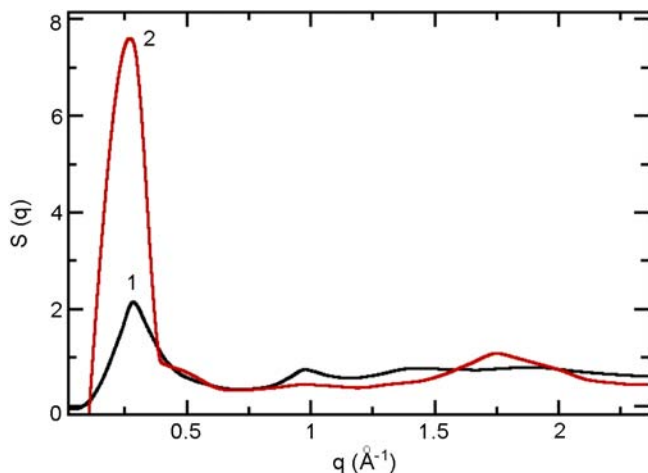


Fig. 4 — Comparison of the total neutron weighted structure factor between systems A and B. [1, system A; 2, system B].

2.24 nm in real space) is the signature of nanoscale ordering in $[\text{C}_{10}\text{mim}]$ cation based ionic liquids. The increase in intensity of this peak in system B indicates a considerable enhancement of spatial heterogeneity in the IL with divalent anion. Molecular dynamics simulations²⁵ have shown that though all the PSFs contribute to the peak at 0.28 \AA^{-1} , some PSFs (such as anion-anion) make greater contribution to it. Figure 5 compares the PSFs between system A and system B.

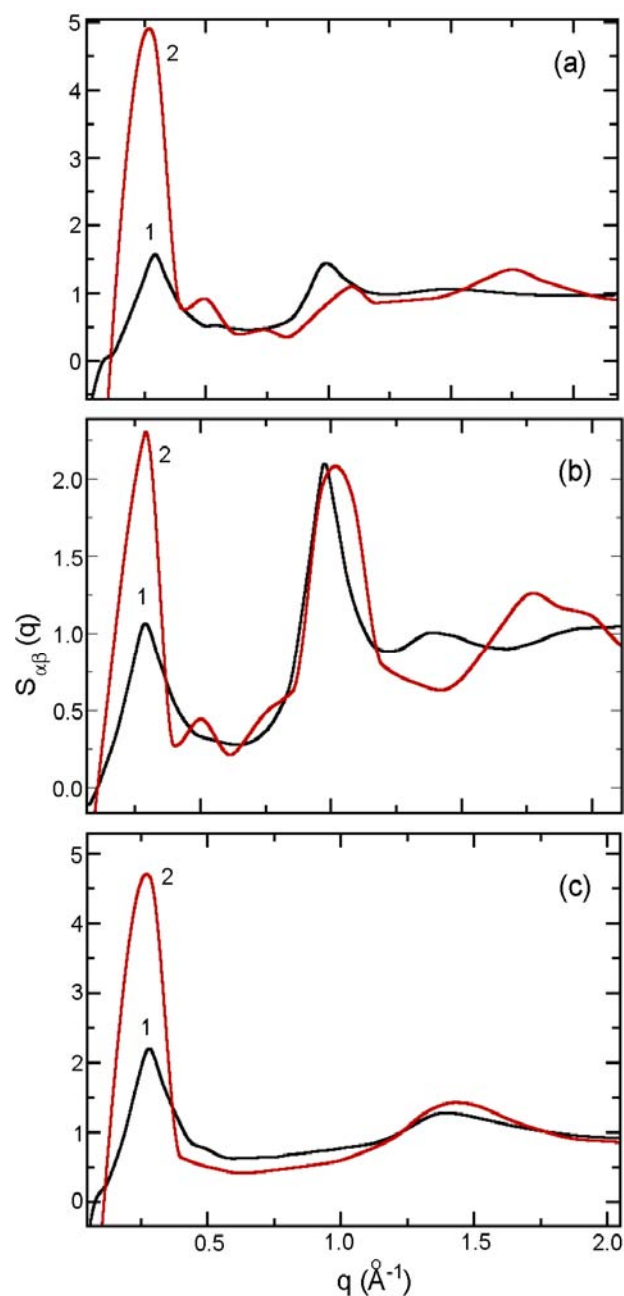


Fig. 5 — Comparison of partial structure factors between systems A and B. [a, II-II; b, PF-PF; c, CT-CT bead pairs. 1, system A; 2, system B].

Compared to system A, all the PSFs of system B have peak at 0.28 \AA^{-1} with larger intensity.

Figure 6 shows a snapshot of system B. A similar figure for system A has been published elsewhere²⁵. Sites forming the polar head (imidazolium ring) of the cation and the anion are shown in red and the non-polar sites of the tail are shown in yellow. These regions are distributed heterogeneously in the ionic liquid.

Figure 4 also indicates that the intensity of the peak at 0.97 \AA^{-1} (6.5 \AA in real space) in system B is lower than that in system A. This feature is related to ring-ring (also called head-head) correlations, as can be identified from the PSF shown in Fig. 5a. The RDF between I1-I1 (head-head) shown in Fig. 2c indicates that the first peak is present at 6.5 \AA in system A, whereas at the same distance in system B, the RDF shows a minimum. Thus, the reciprocal space correlations at this length scale are diminished in system B, relative to system A. This is also corroborated by the anion-anion (PF-PF) RDF shown in Fig. 2b. Since anions in system B have larger charge density than system A, they are farther away from each other and the RDF starts having non-zero values only beyond 6 \AA .

The peak in the wave vector range of 1.4 \AA^{-1} to 2.2 \AA^{-1} corresponds to a real space distance of 2.8 \AA to 4.5 \AA . Greater intensity of this peak in system B as compared to system A indicates a stronger local

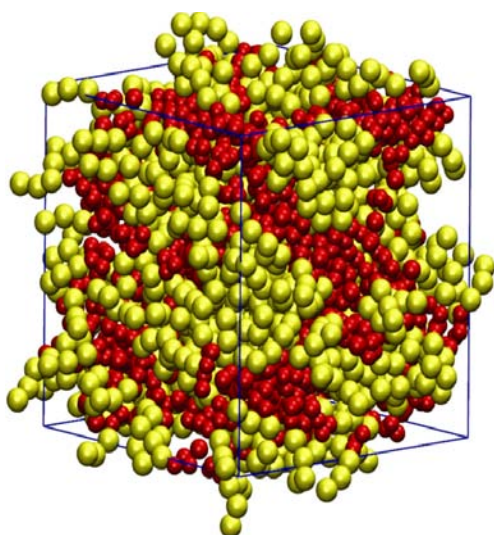


Fig. 6 — Snapshot showing the spatial heterogeneity present in system B (divalent anion). [Beads forming the cation head and anion are in red color and the beads of alkyl chain are in yellow. Length of the simulation box is 55.1 \AA].

structure. This was highlighted by radial distribution functions also.

Dynamics

Coarse grained (CG) models, in general, do not represent the true dynamics of a system. This is so because one employs softer potentials for interaction between beads than the potentials used for interaction between atomic sites in an atomistic MD simulation. Also, the absence of stiff harmonic potentials for bond stretches, angle bends, etc., makes the CG potential energy surface smoother than the rugged landscape characteristic of molecular liquids modelled with atomistic force fields. It is documented by many that CG models often overestimate the diffusion coefficients by two orders of magnitude as compared to atomistic ones³³. Our CG model too shares this trait. Despite the obvious disconnect between the model and experiment (or the real world sample) for dynamical phenomena, we have explored the dynamics of systems A and B. We hope that although their dynamics in individual terms may not be

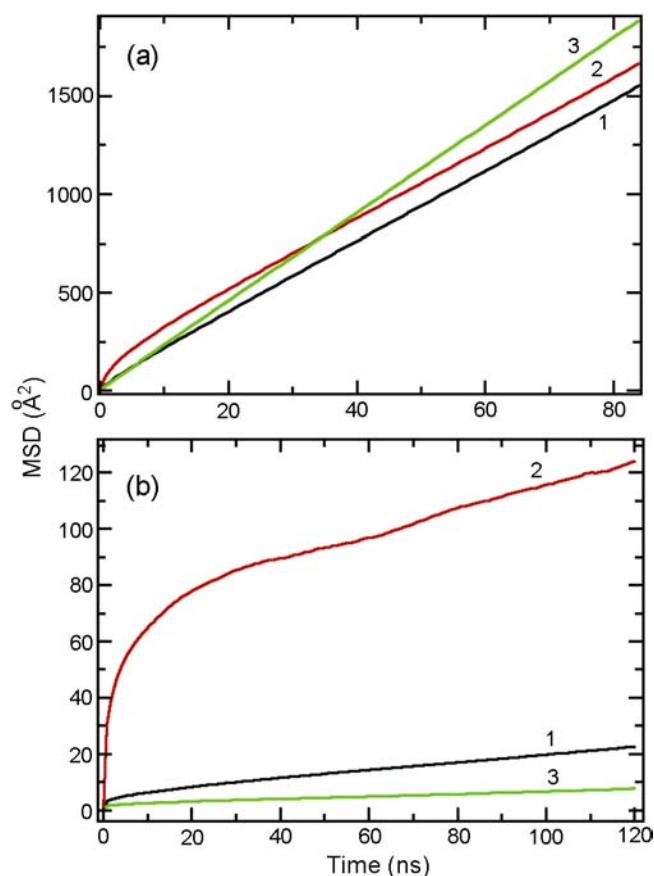


Fig. 7 — Mean squared displacement of head, tail and anion beads. [a, system A; b, system B. 1, head (I1); 2, tail (CT); 3, anion (PF)].

representative of the ionic liquids, the differences between the two systems would be realistic.

We now look at the dynamics of system B and compare it against that of system A. Figure 7 shows the mean squared displacement (MSD) of beads II, CT and PF for systems A and B. The slope of the MSD data gives us an idea about the diffusion coefficient of the beads. In both cases, CT has the highest slope of MSD as compared to II and PF; similar to what is seen in atomistic MD simulations of ILs. While in system A the anions move the fastest (albeit by a small amount), it is the alkyl tail of the cation that shows a large MSD value in system B. System B is characterized by strong electrostatic interactions and thus the polar entities (beads II and PF) diffuse slower than the alkyl tail group. Moreover, the overall MSD values themselves in system B are nearly an order of magnitude smaller than that in system A. The observations of dynamics thus agree with the structural data discussed earlier.

Conclusions

We have carried out coarse grained molecular dynamics simulations of a model ionic liquid—one in which the anions carry twice the charge as that in a traditional ionic liquid. The increase in the anion charge density is compensated by doubling the mole fraction of the cation. A consequence of this change in the potential is an increase in electrostatic interaction between the ions. We have explored the structural and dynamical manifestations of this variation in the interaction potential through coarse grained MD simulations. Our model can be considered to capture the essential features of a room temperature ionic liquid in which the usual monovalent anion is replaced by a divalent one. Our study suggests considerable enhancement of intermolecular structuring, and a more ordered liquid, at all length scales. It will not be surprising, if in reality, such substances are actually crystalline at room temperature – a possibility which is beyond the scope of the current study to explore. The structural microheterogeneity inherent to RTILs with long alkyl tails is vastly amplified in the IL with divalent anions. The substance is also observed to be highly sluggish compared to an IL with a monovalent anion.

Acknowledgement

We thank DST for research grants. SGR thanks CSIR for a research fellowship.

References

- Weingartner H, *Angew Chem Int Ed*, 47 (2008) 654.
- Sheldon R A, *Green Chem*, 7 (2005) 265.
- Welton T, *Chem Rev (Washington, DC)*, 99 (1999) 2071.
- Bhargava B L, Balasubramanian S & Klein M L, *Chem Commun*, (2008) 3339.
- Galinski M, Lewandowski A & Stepniak I, *Electrochim Acta*, 51 (2006) 5567.
- Welton T, *Coord Chem Rev*, 248 (2004) 2459.
- Zhao H, Xia S & Ma P, *J Chem Technol Biotechnol*, 80 (2005) 1089.
- Sarma D & Kumar A, *Appl Catal A: Gen*, 335 (2008) 1.
- Kumar A & Pawar S S, *J Org Chem*, 72 (2007) 8111.
- Kumar A & Pawar S S, *J Mol Catal A: Chem*, 208 (2004) 33.
- Fletcher K A & Pandey S, *J Phys Chem B*, 107 (2003) 13532.
- Sarkar A, Ali M, Baker G A, Tetin S Y, Ruan Q & Pandey S, *J Phys Chem B*, 113 (2009) 3088.
- Schroder C, Hunger J, Stoppa A, Buchner R & Steinhauser O, *J Chem Phys*, 129 (2008) 184501.
- Koddermann T, Wertz C & Ludwig R, *Angew Chem, Int Ed*, 45 (2006) 3695.
- Cammarata L, Kazarian S G, Salter P A & Welton T, *Phys Chem Chem Phys*, 3 (2001) 5192.
- Raju S G & Balasubramanian S, *J Phys Chem B*, 113 (2009) 4799.
- Adhikari A, Dey S, Das D K, Mandal U, Ghosh S & Bhattacharyya K, *J Phys Chem B*, 112 (2008) 6350.
- Dey S, Adhikari A, Das D K, Sasmal D K & Bhattacharyya K, *J Phys Chem B*, 113 (2009) 959.
- Adhikari A, Sahu K, Dey S, Ghosh S, Mandal U & Bhattacharyya K, *J Phys Chem B*, 111 (1997) 12809.
- Urahata S M & Rebeiro M C C, *J Chem Phys*, 120 (2004) 1855.
- Wang Y & Voth G A, *J Am Chem Soc*, 127 (2005) 12192.
- Hu Z & Margulis C J, *Proc Natl Acad Sci*, 103 (2006) 831.
- Wang Y & Voth G A, *J Phys Chem B*, 110 (2006) 18601.
- Lopes J N C & Padua A A H, *J Phys Chem B*, 110 (2006) 3330.
- Bhargava B L, Devane R, Klein M L & Balasubramanian S, *Soft Matt*, 3 (2007) 1395.
- Mandal P, Sarkar M & Samanta A, *J Phys Chem A*, 108 (2004) 9048.
- Paul A, Mandal P K & Samanta A, *J Phys Chem B*, 109 (2005) 9148.
- Triolo A, Russina O, Bleif H & Di Cola E, *J Phys Chem B*, 111 (2007) 4641.
- Triolo A, Russina O, Fazio B, Triolo R & Di Cola E, *Chem Phys Lett*, 457 (2008) 362.
- Raju S G & Balasubramanian S, *J Phys: Cond Matt*, 21 (2009) 35105.
- Raju S G & Balasubramanian S, *J Mater Chem*, 19 (2009) 4343.
- Plimpton S J, *J Comp Phys*, 117 (1995) 1.
- Nielsen S O, Lopez C F, Srinivas G & Klein M L, *J Phys Cond Matt*, 16 (2004) R481.